ACS Sustainable Chemistry & Engineering

Research Article

pubs.acs.org/journal/ascecg

The Role of Composition for Cobalt Molybdenum Carbide in Ammonia Synthesis

Ihfaf AlShibane,[†] Angela Daisley,[†] Justin S. J. Hargreaves,*[,†] Andrew L. Hector,[‡] Said Laassiri,[†] Jose L. Rico,[§] and Ronald I. Smith[∥]

[†]WestCHEM, School of Chemistry, University of Glasgow, Joseph Black Building, Glasgow G12 8QQ, United Kingdom

[‡]Chemistry, University of Southampton, Southampton SO17 1BJ, United Kingdom

[§]Laboratorio de Catálisis, Facultad de Ingeniería Química, Universidad Michoacana de San Nicolás de Hidalgo, Edificio V1, CU, C.P., 58060 Morelia, Michoacán, Mexico

[∥]ISIS Facility, Rutherford Appleton Laboratory, Chilton, Didcot OX11 0QX, United Kingdom

ABSTRACT: The performance of Co_3Mo_3N, Co_3Mo_3C, and Co_6Mo_6C for ammonia synthesis has been compared. In contrast to Co_3Mo_3N, which is active at 400 °C, a reaction temperature of 500 °C, which was preceded by an induction period, was necessary for the establishment of steady state activity for Co_3Mo_3C. Co_6Mo_6C was found to be inactive under the conditions tested. During the induction period, nitridation of the Co_3Mo_3C lattice was found to occur, and this continued throughout the period of steady state reaction with the material transforming in composition toward Co_3Mo_3N. Taken together, these observations demonstrate that ammonia synthesis activity in ternary cobalt molybdenum systems is associated with the presence of N in the 16c Wyckoff lattice site.

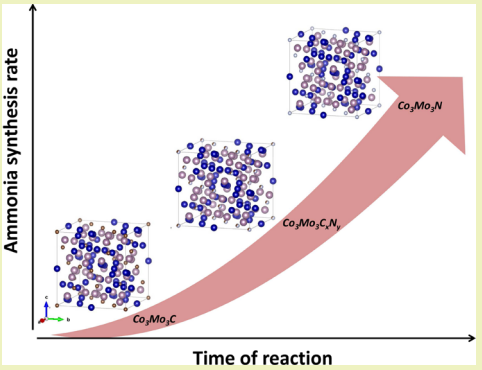

KEYWORDS: *Ammonia synthesis, Mars-van Krevelen, Co_3Mo_3N, Co_3Mo_3C, In situ neutron diffraction*

INTRODUCTION

The development of the Haber−Bosch Process for the industrial-scale synthesis of ammonia from N_2 and H_2 feedstock was a landmark 20th century achievement.[1] This process employs an iron-based catalyst and is operated at very high pressure (>100 atm) and moderate temperatures (ca. 400 °C) to accomplish acceptable process yields. It is also necessary to use highly pure feed gases. Taking the whole process into consideration (including the generation of feedstock), as operated on the industrial scale, the process is currently responsible for ca. 1−2% of global energy demand producing more than 1.5 tonnes of CO_2 per tonne of NH_3 made.[2] While the process is well integrated and iron is a widely abundant and cheap catalyst which exhibits, under the correct conditions, a significant lifetime, the search for new catalytic materials and/or processes for ammonia synthesis is an area of topical interest. A strong driver for this is the development of routes with enhanced sustainability and/or facilitating more localized production requiring smaller distribution networks. On the industrial scale, a more highly active carbon-supported ruthenium-based catalyst was developed, and it forms the basis of the Kellogg Advanced Ammonia Process (KAAP). To date, while there has been some industrial uptake of this system, this has been limited. The development of this ruthenium catalyst has recently been outlined.[3] Given the fact that thermodynamically ammonia synthesis is favored by lower reaction temperatures, the development of more active catalysts which could lead to exploitation of this thermodynamic window and a concomitant reduction in the severity of the conditions required for operation of ammonia synthesis continues to be a major focus of attention. The performance of a number of different materials has been reported in the literature including Co_3Mo_3N,[4,5] Ni_2Mo_3N,[4,6] Co-Re,[7,8] BaH_2/Co,[9] Ru/electride,[10] and lithium hydride−transition metal (nitride) combinations.[11] In making an activity comparison between the Fe-K_2O-Al_2O_3 and Co_3Mo_3N catalysts at atmospheric pressure and 400 °C, Kojima and Aika have reported rates of 330 and 652 μmol h^{-1} g^{-1}, respectively,[5] and in a study at elevated pressure and with a feed containing ammonia, Jacobsen has also reported the Co_3Mo_3N to exhibit better ammonia synthesis performance than a commercial multipromoted iron catalyst.[4]

Among the different systems investigated, we have been interested in the possibility that Mars−van Krevelen mechanisms may be operative for metal nitrides.[12] To this end, the reactivity of lattice N in Co_3Mo_3N with hydrogen has been investigated where it was found that some NH_3 could be produced in the absence of gas-phase N_2.[13,14] Furthermore, at elevated reaction temperature, 50% loss of lattice N occurred resulting in the η-12 carbide-structured Co_6Mo_6N phase, which was previously unprecedented.[15] The residual lattice N was

Received: June 30, 2017
Revised: August 15, 2017
Published: August 23, 2017

DOI: 10.1021/acssuschemeng.7b02168
ACS Sustainable Chem. Eng. 2017, 5, 9214−9222

found to relocate from the original 16c Wyckoff site in Co_3Mo_3N in which it is coordinated to six Mo species in a slightly distorted octahedron to the 8a site in Co_6Mo_6N in which coordination to six Mo species in a nondistorted octahedron occurs.[16] The possible occurrence of a Mars–van Krevelen mechanism was also demonstrated in nitrogen isotopic exchange measurements where lattice N was found to exchange with $^{15}N_2$, with the extent of exchange being a strong function of the pretreatment of the material.[17] Recent computational modeling has indicated the occurrence of significant concentrations of surface N vacancies at the (111) surface of Co_3Mo_3N under conditions of relevance to the ammonia synthesis reaction.[18] In addition, the activation of N_2 and H_2 at a range of surface sites has also been probed.[19] As well as providing a pathway for ammonia synthesis, the possible occurrence of N-centered Mars–van Krevelen-based mechanisms could also be of relevance for the development of N-looping systems. In such systems, the lattice nitrogen present in a nitride can be directly reacted to form a product, for example, a nitrogen-containing organic molecule, generating vacancies. These vacancies can then be replenished in a separate step possibly which, if necessary, can be conducted at a different temperature.[12] Related approaches have recently been investigated for solar nitrogen fixation[20,21] as well as two-stage NH_3 generation.[22,23] In addition to more conventional heterogeneous catalysis and N-looping, the possible occurrence of the Mars–van Krevelen-based mechanism has recently been the subject of computational modeling in relation to the application of nitride-based electrocatalysts for the generation of ammonia.[24,25]

In the current study, the catalytic performance of Co_3Mo_3C and Co_6Mo_6C for ammonia synthesis is investigated. The particular interest in these systems arises from the high efficacy of Co_3Mo_3N for ammonia synthesis as documented above. Furthermore, the phase transformation between Co_6Mo_6N and Co_3Mo_3N is known to be very favorable under the ammonia synthesis conditions employed in this study,[26] and it is of interest to see the extent to which the Co_6Mo_6C exhibits related behavior. By undertaking such a study and benchmarking it against the performance of the corresponding nitrides, further information on the requirement for lattice N, a necessary component for Mars–van Krevelen ammonia synthesis, can be probed.

EXPERIMENTAL SECTION

Materials Preparation. $CoMoO_4$ was prepared as described elsewhere.[13] In summary, the required quantities of $(NH_4)_6Mo_7O_{24}.4H_2O$ (99.98%, Sigma-Aldrich) and $Co(NO_3)_2.6H_2O$ (>98%, Sigma-Aldrich) were dissolved in deionized water. The solution was then heated to 85 °C and held at this temperature for 5 h. The resulting purple precipitate was filtered and washed with distilled water and ethanol. The precipitate was then calcined at 500 °C for 5 h.

Co_3Mo_3N was prepared by ammonolysis of $CoMoO_4$ under NH_3 (BOC, 99.98%) at a flow rate of 100 mL min^{-1} at 785 °C for 5 h. The ramp rate applied was that the temperature was increased from ambient to 357 °C at 5.6 °C min^{-1}, then after to 447 °C min^{-1} at 0.2 °C min^{-1} before being finally increased to 785 °C at 2.1 °C min^{-1}.

Co_3Mo_3C was prepared by the carburization of Co_3Mo_3N under 20 vol % CH_4 in H_2 (BOC, 99.98%) at a flow rate of 12 mL min^{-1} at 700 °C for 2 h with a ramp rate of 6 °C min^{-1} to reach 350 °C followed by 1 °C min^{-1} to attain 700 °C.

Co_6Mo_6C was prepared by reducing Co_3Mo_3C under 75 vol % H_2 in Ar (BOC, 99.98%) at a flow rate of 60 mL min^{-1}. The reduction was conducted at 900 °C for 5 h.

Materials Characterization. *X-ray Diffraction.* Diffraction patterns were collected on a Siemens D5000 instrument, using Cu Kα radiation (λ = 0.154 nm) over a 2θ range of 10°–80°, a step size of 0.02°, and a counting time of 1s per step. Samples were prepared by compaction into a Si sample holder. Phase identification was obtained by comparison with JCPDS database files.

In Situ Powder Neutron Diffraction (PND). *In situ* controlled atmosphere high temperature time-of-flight (ToF) PND data was collected using the high intensity Polaris diffractometer at the ISIS pulsed spallation source (Rutherford Appleton Laboratory, UK). Powder samples (ca. 1 g) were loaded into 11 mm diameter thin-walled stainless steel cells and held in place between quartz glass frits to permit a flow of reaction gas to circulate through the samples during data collection. The cell assembly was mounted in a dedicated neutron diffraction furnace capable of heating it from room temperature to ~900 °C and connected to a gas panel fitted with mass flow controllers allowing a mixture of gases to flow through the sample at controlled flow rates during data collection. A collimator manufactured from neutron-absorbing boron nitride ceramic placed around the cell enabled diffraction patterns to be collected in the Polaris 2$\theta \approx 90°$ detector bank which were free of Bragg reflections from the steel walls of the cell. Rietveld refinements against PND data were performed using the General Structure Analysis System (GSAS) through the EXPGUI interface.[27,28]

Surface Area Measurement. Surface areas were determined from N_2 physisorption isotherms collected at −196 °C upon samples previously degassed at 110 °C under vacuum for 12 h. The specific surface area, S_{BET}, was calculated by applying the BET method.

Scanning Electron Microscopy. Scanning electron microscopy was performed on Philips XLSEM and FEI Quanta 200F Environmental instruments operating at 20 kV. To limit the deleterious effect of charging, samples were coated with an Au/Pd alloy before imaging.

Elemental analysis. Nitrogen analysis was undertaken by combustion using an Exeter Analytical CE-440 Elemental Analyzer.

Catalytic Activity Tests. Reactions were performed using 0.3 g of material under an atmosphere of 75 vol % H_2 in N_2 (BOC, 99.98%) at ambient pressure employing a total gas feed of 60 mL min^{-1}. Ammonia production was determined by measurement of the decrease in the conductivity of 200 mL of a 0.0018 M H_2SO_4 solution through which the reactor effluent stream flowed. Details of the reactor have been presented elsewhere.[6] Error propagation calculations have been performed and reported for each experiment

RESULTS AND DISCUSSION

Structural and Textural Properties of Molybdenum Cobalt-Based Materials. The structural and textural properties of the CoMo based materials following the different nitridation and carburization processes were monitored using XRD analysis, neutron diffraction, and SEM as presented in Figures 1–4. Table 1 summarizes some of the physicochemical features of the prepared materials.

Preparation of Co_3Mo_3N. Prior to the preparation of Co_3Mo_3N, the synthesis of a single-phase cobalt molybdate, considered as the precursor for nitridation, was confirmed by XRD analysis (Figure 1(a)). The $CoMoO_4$ exhibited intense and sharp reflections indicative of a well-crystallized material. All the observed reflections belong to the dehydrated $CoMoO_4$ phase (PDF number: 00-021-0868). Following ammonolysis, a single phase corresponding to Co_3Mo_3N was obtained. The XRD pattern (Figure 1(b)) showed intense and sharp reflections that belonged exclusively to the Co_3Mo_3N phase (PDF number: 01-089-7953) suggesting the preparation of a well-crystallized nitride phase. The neutron diffraction pattern collected after the nitridation step was also consistent with the formation of Co_3Mo_3N. The Co_3Mo_3N structure derived from the Rietveld refinement corresponded to the η-6 carbide structure as reported previously by zur Loye and co-workers.[29]

DOI: 10.1021/acssuschemeng.7b02168
ACS Sustainable Chem. Eng. 2017, 5, 9214–9222

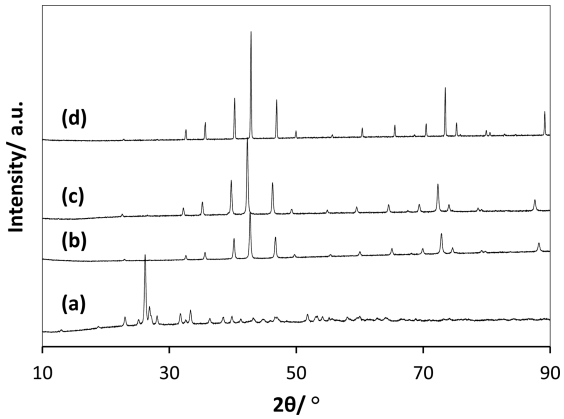

Figure 1. PXRD patterns collected on the as prepared cobalt molybdenum materials: (a) $CoMoO_4$, (b) Co_3Mo_3N, (c) Co_3Mo_3C, and (d) Co_6Mo_6C.

The refined structural parameters are listed in Table 2, and the observed and calculated diffraction profiles are shown in Figure 2(a). The nitrogen content of this material has been determined by elemental analysis to be 3.0 ± 0.1 wt %, which is consistent with the theoretical value of 2.9 wt % for Co_3Mo_3N (Table 1).

Preparation of Co_3Mo_3C. The XRD pattern collected after the carburization of Co_3Mo_3N in the conditions described above is presented in Figure 1(c). The XRD pattern of Co_3Mo_3C was similar to Co_3Mo_3N, and only a small shift toward lower 2θ was observed for all reflection peaks, indicating that both materials have the same space group ($Fd\bar{3}m$) but with different cell parameters due to nitrogen substitution by carbon. Rietveld structure refinement with the neutron diffraction data resulted in the lattice parameters shown in Table 2 and confirmed the η-6 carbide structure of Co_3Mo_3C. All the observed reflections, except the two at d = 1.752 and 2.032 Å which relate to the *in situ* reaction cell and which were consequently not included in the refinement, belonged to the Co_3Mo_3C phase. The observed lattice parameter (a = 11.0576(2) Å) matches reasonably well with the reported value for Co_3Mo_3C (a = 11.0709(3) Å).[30] The elemental analysis showed that the carbon content (2.5 ± 0.1 wt %) accords well with the theoretical value of 2.5 wt % expected for Co_3Mo_3C. In addition, no nitrogen was found to be present in this material.

Preparation of Co_6Mo_6C. The reduction of Co_3Mo_3C at 900 °C resulted in the formation of Co_6Mo_6C. The XRD pattern collected after the reaction was similar to the parent material with the exception of a noticeable shift of all reflections to higher 2θ. Co_6Mo_6C and Co_3Mo_3C crystallize in the same space group (Table 2). In the Co_6Mo_6C structure, the carbon species is solely located in the 0 0 0 (8a) sites and the $^1/_8$ $^1/_8$ $^1/_8$ (16c) sites are vacant, whereas for Co_3Mo_3C the opposite is the case. This difference in the lattice parameter is easily observed in our case when the XRD patterns of Co_6Mo_6C and Co_3Mo_3C are compared (Figures 1(c) and (d)). Results from room temperature PND supported the preparation of a pure Co_6Mo_6C phase (a = 10.9071(1) Å, Table 2) and confirmed the XRD observation. Elemental analysis confirmed the reduction of carbon content to 1.3 ± 0.1 wt % which corresponds to the theoretical value expected (1.3 wt %).

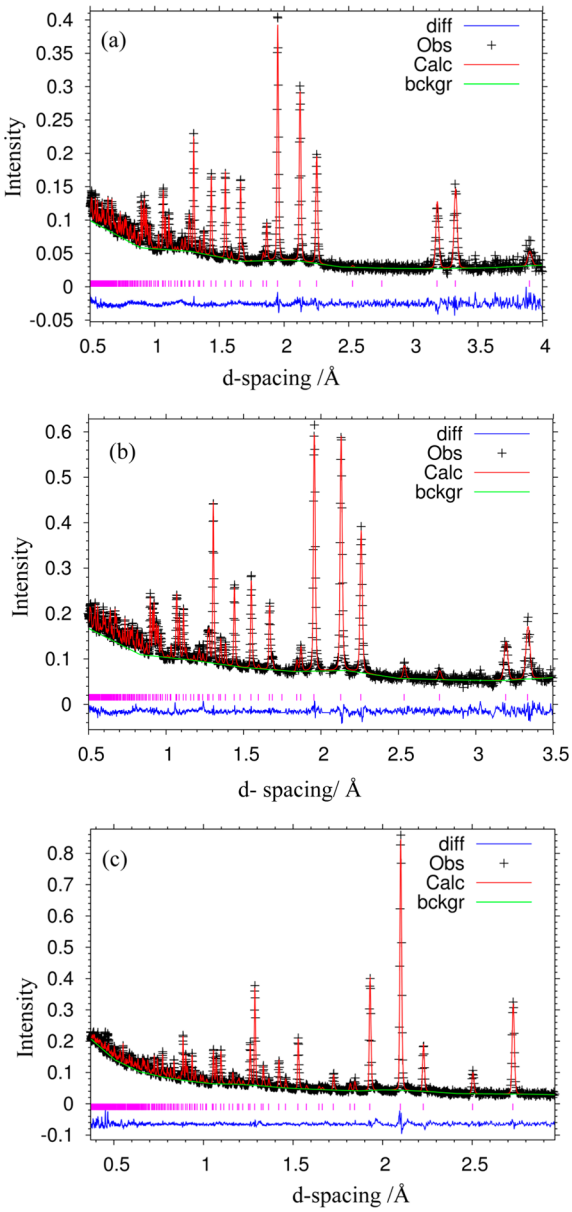

Figure 2. Fitted powder neutron diffraction profiles from Rietveld refinement for the as prepared materials: (a) Co_3Mo_3N, (b) Co_3Mo_3C, and (c) Co_6Mo_6C.

The morphology of all the prepared samples was investigated by scanning electron microscopy (SEM), and representative micrographs are presented in Figure 3. The morphology of the different samples ($CoMoO_4$, Co_3Mo_3N, Co_3Mo_3C, and the Co_6Mo_6C) is similar, being in the form of aggregated needles, indicating that the nitridation and carburization processes are pseudomorphic as expected from previous literature.[31] The relatively sharp XRD reflections (Figure 1) are indicative that the materials are, in general, well ordered and comprise large coherent diffraction domains. The latter is consistent with the low surface areas exhibited being 7, 18, and 13 m^2 g^{-1} for $CoMoO_4$, Co_3Mo_3N, and Co_3Mo_3C respectively (Table 1). The surface area of Co_6Mo_6C was particularly low being ~3 m^2 g^{-1}, which can be attributed to the influence of the very high reaction temperature employed in its preparation.

Catalytic Activity of Molybdenum Cobalt-Based Materials. The role of the lattice nitrogen in the catalytic

DOI: 10.1021/acssuschemeng.7b02168
ACS Sustainable Chem. Eng. 2017, 5, 9214−9222

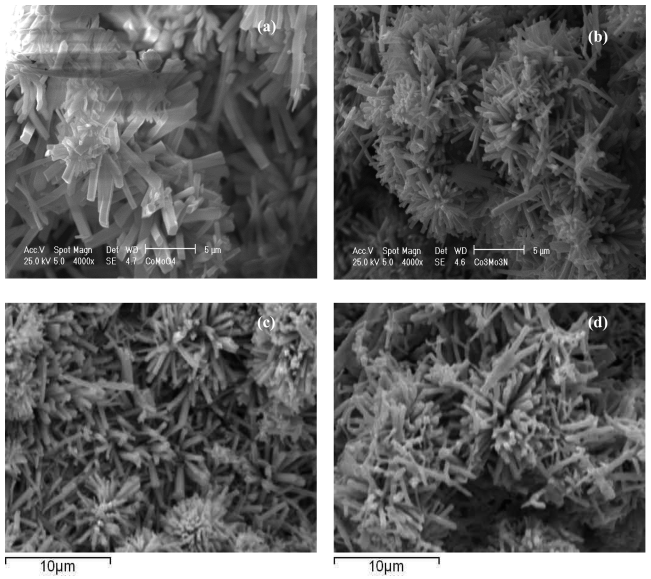

Figure 3. SEM images of as prepared materials: (a) $CoMoO_4$ (b) Co_3Mo_3N (c) Co_3Mo_3C and (d) Co_6Mo_6C.

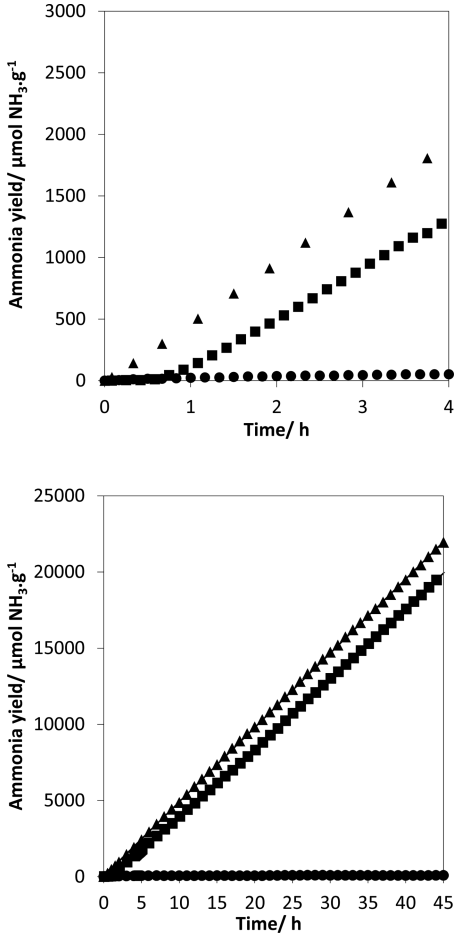

Figure 4. Ammonia yield of CoMo related materials under 60 mL min^{-1} of 75 vol % H_2 in N_2 (BOC, 99.98%) at 500 °C: (▲) Co_3Mo_3N, (■) Co_3Mo_3C, and (●) Co_6Mo_6C.

activity was studied by comparing the results of Co_3Mo_3C and Co_6Mo_6C for ammonia synthesis to the well-established activity of the Co_3Mo_3N system. Figure 4 shows the evolution of ammonia at 500 °C as a function of time under an atmosphere of 75 vol % H_2 in N_2 (BOC, 99.98%) at a total gas feed of 60 mL min^{-1}.

As expected, the Co_3Mo_3N system was found to be highly active for ammonia synthesis at ambient pressure (Figure 4) exhibiting a rate of ca. 489 μmol g^{-1} h^{-1} (Table 3) which can be compared to ca. 690 μmol g^{-1} h^{-1} which would correspond to the thermodynamically limited yield of 0.129%. Under the same reaction conditions, the Co_3Mo_3C system displayed a comparable activity to Co_3Mo_3N (461 μmol g^{-1} h^{-1}, Table 3). However, this was only exhibited after an induction time of ca. 40 min, during which the material demonstrated very poor activity (Figure 4) and beyond which the material exhibited steady state performance during 45 h of reaction with no sign of deactivation. It is noteworthy that Co_3Mo_3C was found to be inactive at 400 °C, a temperature at which Co_3Mo_3N is known to be highly active.[5] In the case of Co_6Mo_6C, the material was found to be inactive at 500 °C even upon extended times on stream.

The induction time, during which the activity "switched-on", was only observed in the case of Co_3Mo_3C and implies that the material undergoes structural/surface changes that lead to the formation of an active phase. Consequently, this aspect was further investigated.

Evolution of Co_3Mo_3C Phase and Structure under Ammonia Synthesis Conditions. Figure 5 presents selected *in situ* neutron diffraction patterns collected at different temperatures and at 500 °C at different reaction times for the Co_3Mo_3C material. All the patterns were analyzed by the Rietveld method using the η-6 carbide Co_3Mo_3C structure as the starting model. The evolution of the lattice parameter during the different stages of reaction is presented in Figure 5.

When increasing the temperature to 500 °C, a linear change of lattice parameter as a function of temperature was generally observed. This can be attributed to thermal expansion of the lattice. However, a change in the slope was detected at temperatures ranging between 400 and 500 °C, which could relate to structural transformation. At 500 °C, no variation of the lattice parameters was observed within the first 10 min of reaction. Thereafter, a gradual contraction of the lattice with reaction time was detected. In addition to lattice parameter determination, the difference in neutron scattering lengths of carbon (6.646 fm) and nitrogen (9.36 fm) is sufficiently large to allow the assessment of the C/N substitution. The evolution of the C/N occupancy at the 16c Wyckoff lattice site as a function of reaction time at 500 °C is presented in Figure 6. Gradual substitution of carbon with nitrogen under reaction conditions is evident.

Following 2 h of reaction at 500 °C, the sample temperature was decreased to room temperature under the same reaction atmosphere, and a long neutron diffraction run was then performed. Initially, an attempt was made to refine the structure to the Co_3Mo_3C model for this sample. However, the atomic displacement parameters were unrealistic. Instead, very good agreement was obtained when the structure was refined against the Co_3Mo_3N reference (Figure 7 and Table 4). The lattice parameter derived from Rietveld refinement with the neutron diffraction data was found to be a = 11.0370(3) Å, falling between the lattice parameter observed for Co_3Mo_3C (a = 11.0576(2)) and Co_3Mo_3N (a = 11.0245(7)) as presented in Table 1. An estimated chemical composition of $Co_3Mo_3C_{0.38}N_{0.62}$ was calculated applying Vegard's law. This was further confirmed by elemental analysis. Furthermore,

DOI: 10.1021/acssuschemeng.7b02168
ACS Sustainable Chem. Eng. 2017, 5, 9214−9222

Table 1. Physicochemical Properties of Molybdenum Cobalt-Based Materials

			Chemical composition			
	BET[a]/m^2 g^{-1}	XRD Phase	Co[b]/wt %	Mo[b]/wt %	C[c]/wt %	N[c]/wt %
$CoMoO_4$	7	(00-021-0868)	22.8	39.6	–	–
Co_3Mo_3N	18	(01-089-7953)	35.2	59.1	–	3.0 ± 0.1
Co_3Mo_3C	13	(03-065-7128)	28.5	53.9	2.5 ± 0.1	–
Co_6Mo_6C	3	(03-065-8115)	33.2	53.6	1.3 ± 0.1	–

[a]S_{BET} is the specific surface area evaluated using the BET method. [b]Analysis by EDX. [c]Determined by elemental analysis.

Table 2. Summary of Crystallographic Parameters of As-Prepared Molybdenum Cobalt-Based Materials Derived from Room Temperature Neutron Diffraction Data

	Co_3Mo_3N	Co_3Mo_3C	Co_6Mo_6C
Crystal system	Cubic	Cubic	Cubic
Space group	$Fd\bar{3}\ m$	$Fd\bar{3}\ m$	$Fd\bar{3}\ m$
Cell parameter a/Å	11.0245(7)	11.0576(2)	10.9071(1)
Unit-cell volume/Å^3	1339.94(5)	1352.03(6)	1297.57(5)
Rp	0.0540	0.0327	0.0569
wRp	0.0358	0.0413	0.0490
χ^2	1.529	2.111	2.301

Table 3. Summary of Nitrogen Reactivity of CoMo-Based Materials under 60 mL min^{-1} of 75 vol % H_2 in N_2 (BOC, 99.98%) at 500°C

	Co_3Mo_3N	Co_3Mo_3C	Co_6Mo_6C
Ammonia synthesis rate/ μmol g^{-1} h^{-1}	489 ± 17	461 ± 17	n.d.[a]

[a]n.d.: no measurable amount of ammonia was detected.

refining the C/N mixing in the 16c Wyckoff lattice leads to a ratio of 0.33(5)/0.66(4), again similar to the composition estimated using Vegard's law, revealing a significant carbon substitution by nitrogen during ammonia synthesis (Table 4). To ascertain the evolution of the chemical composition of the Co_3Mo_3C during ammonia synthesis reaction at 500 °C, elemental analysis of postreaction material was conducted after different times on stream (Figure 8). The gradual substitution of carbon with nitrogen was observed, and close to complete carbon substitution occurred after 48 h of reaction (C: 0.31 ± 0.1 wt % and N: 2.5 ± 0.1 wt %). Moreover, postreaction XRD analysis conducted after 48 h of reaction (Figure 9) confirmed the conversion of Co_3Mo_3C to a material of composition close to Co_3Mo_3N. Postreaction SEM analysis demonstrated that, as anticipated, morphology was unaffected by reaction (Figure 10).

In contrast to Co_3Mo_3C, elemental analysis did not reveal any nitrogen insertion in the structure of Co_6Mo_6C after the ammonia synthesis reaction test conducted at 500 °C. To probe the possibility that the low surface area of Co_6Mo_6C (ca. 3 m^2 g^{-1}) was responsible for the limited incorporation of lattice N, the material was kept under reaction conditions for 48 h. However, no nitrogen incorporation was observed, and the resultant phase observed by XRD corresponded to that expected for Co_6Mo_6C (Figure 11). The stability of the Co_6Mo_6C phase during ammonia synthesis reaction might explain the inactivity of this material for ammonia generation, in that the development of activity might be associated with the formation of an active nitride or carbonitride phase.

DISCUSSION

When considered in the context of their related structures, it is interesting to make direct comparisons between performance of the nitride and the two carbide materials. Within the literature, the efficacy of Co_3Mo_3N for ammonia synthesis has been attributed to the combination of the Co and Mo components having a close to optimal binding energy for N_2.[32] In this model, it has been proposed that the active crystallographic face of the material is the (111) termination plane which expresses both Co and Mo. It was also proposed that the interstitial nitrogen is not active in itself but instead maintains the required crystallographic ordering. Alternatively, it has been proposed by some of the current authors that Co_3Mo_3N might operate via the Mars–van Krevelen mechanism in which the catalytic lattice nitrogen is hydrogenated to yield NH_3 and a lattice vacancy. This vacancy is subsequently replenished from N_2 with further hydrogenation of the resultant lattice N species continuing the catalytic cycle. There have been both experimental and modeling based studies which support this viewpoint.[12−19] In the current study it is noted that, unlike Co_3Mo_3N, both carbides are inactive at 400 °C. In fact, Co_6Mo_6C does not demonstrate any detectable activity under any of the conditions tested. Structure sensitivity, as arising from the suggestion of the (111) surface plane being predicted to be the active termination plane, has yet to be experimentally demonstrated in the Co_3Mo_3N system; in the current investigation the SEM studies (Figure 3) indicate the gross morphology to be similar for all the materials tested. On this basis, there is strong evidence that the influence of difference in morphology can be discounted as the origin of the observed difference in catalytic performance and that rather it is the difference in composition between Co_3Mo_3N and Co_3Mo_3C that might be determining. Indeed, it is the case that the lag period associated with the development of activity in the case of the carbide corresponds to the further replacement of lattice C with N. This would be consistent with the operation of a Mars–van Krevelen mechanism in which lattice nitrogen has to be present for ammonia synthesis to occur once a critical population of lattice N was established. However, a degree of caution is necessary in drawing this tentative conclusion since it has yet to be established whether there is a complicating role of *in situ* removal of the passivation layer[33] during reaction which could conceivably occur to different extents for the two materials, and it has yet to be definitively established whether the nitridation of the carbide lattice precedes ammonia synthesis or indeed results from it. It is, however, noteworthy that upon attaining 500 °C under the reaction mixture the lattice partially nitrides (the nitrogen content for a sample cooled under the mixture immediately upon attaining 500 °C was ∼0.4 wt %) which suggests that a critical degree of N incorporation into the material may be required for the development of activity since at this stage the material does not

DOI: 10.1021/acssuschemeng.7b02168
ACS Sustainable Chem. Eng. 2017, 5, 9214−9222

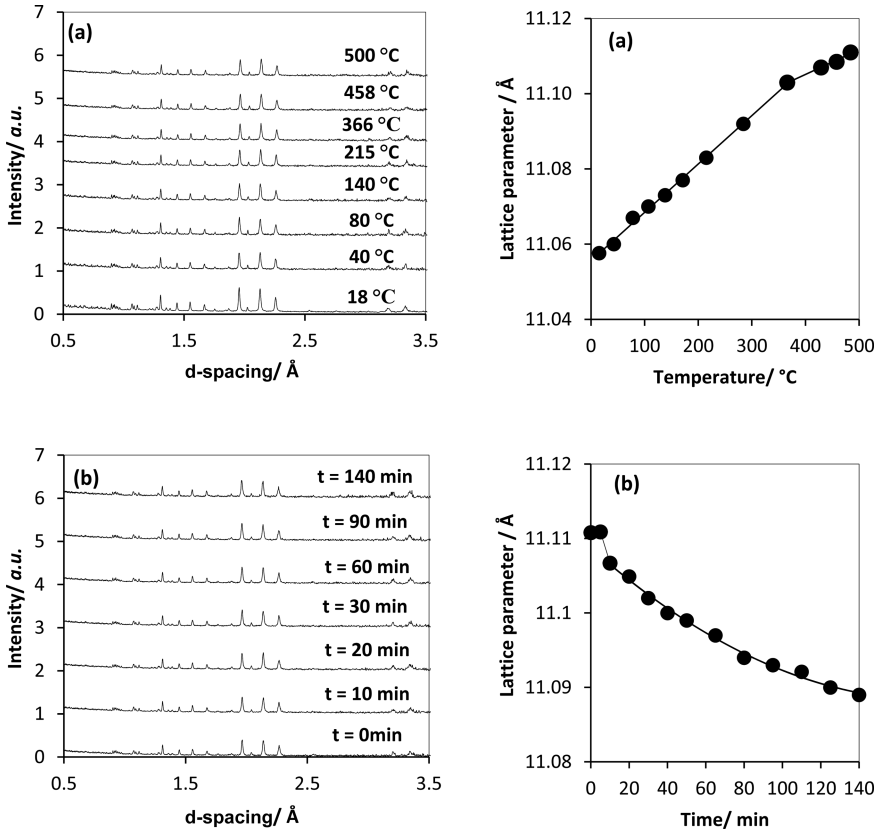

Figure 5. Diffraction patterns and evolution of the lattice parameter of Co_3Mo_3C during the ammonia synthesis reaction as a function of temperature and time: (a) temperature-programmed reaction and (b) isothermal conditions at 500 °C. *In situ* measurements were conducted under 60 mL min^{-1} 75 vol % H_2 in N_2 (BOC, 99.98%) .

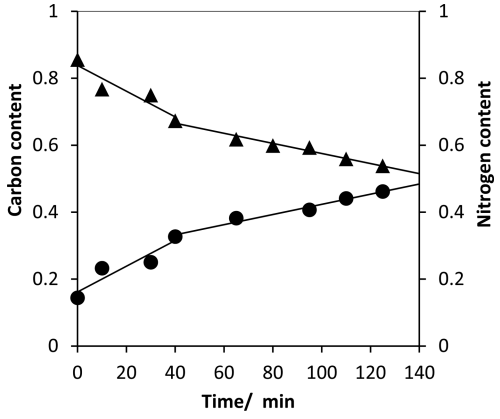

Figure 6. Evolution of the C/N occupancy of the 16c Wyckoff lattice site in Co_3Mo_3C as a function of reaction time with 60 mL min^{-1} of 75 vol % H_2 in N_2 (BOC, 99.98%) at 500 °C. (▲) Fractional carbon content and (●) fractional nitrogen content as determined from the Rietveld refinement against powder neutron diffraction data.

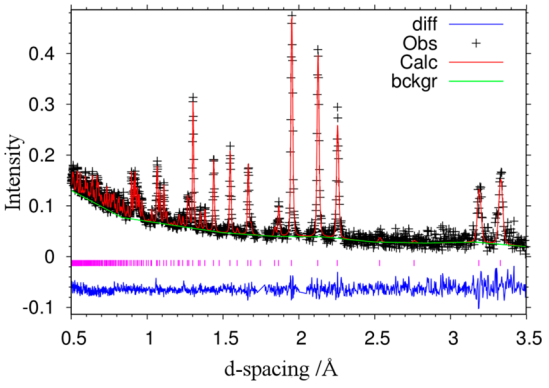

Figure 7. Fitted powder neutron diffraction profile from Rietveld refinement against powder neutron diffraction data for Co_3Mo_3C after 2 h of reaction with 60 mL min^{-1} of 75 vol % H_2 in N_2 (BOC, 99.98%) at 500 °C.

apparently produce detectable quantities of ammonia. The reaction profile could be consistent with a surface reconstruction to yield an active surface plane occurring upon attainment of a critical nitrogen content within the material which might explain the sudden onset of activity as a function of time on stream. It is also noteworthy that beyond the induction period, given the steady state nature of the reaction, the performance of the material does not further change with increasing lattice nitrogen content thereby demonstrating that a material close in composition to Co_3Mo_3N (as evident after 48 h on stream) and the intermediate carbonitride materials exhibit equivalent performance. In the case of Co_3Mo_3C, which develops activity as a function of time, and Co_6Mo_6C which does not produce ammonia or nitride even on prolonged reaction, the effect of the passivation layer would be expected to be less of a consideration due to the close chemical similarity of the materials. On this basis, it seems that the subtle difference in crystallography, with the former material containing twice the carbon content of the latter and in a different crystallographic site (i.e., the 16c Wyckoff site as opposed to the 8a site), is determining. In this respect, it is interesting to note the comparative enhanced stability of carbides with respect to

DOI: 10.1021/acssuschemeng.7b02168
ACS Sustainable Chem. Eng. 2017, 5, 9214−9222

Table 4. Structure Parameters of Co_3Mo_3C after 2 h of Reaction with 60 mL min^{-1} of 75 vol % H_2 in N_2 (BOC, 99.98%) at 500°C Obtained from Neutron Diffraction Data

Atom	Site	Occupancies	x	y	z	U_{iso}/Å^2
Co	48f	1.000	0.2936(3)	0.2936(3)	0.2936(3)	0.0011(9)
Co	32e	1.000	0.5	0.5	0.5	0.0019(1)
Mo	16d	1.000	0.3237(4)	0.125	0.125	0.0019(3)
N	16c	0.66(4)	0	0	0	0.0065(3)
C	16c	0.33(5)	0	0	0	0.0065(3)

[a]Space group $Fd\bar{3}mZ$ (227); a = 11.0370(3) Å, V = 1344.5(2) Å^3, R_{wp} = 0.0624, R_p = 0.1001, χ_{red}^2 = 0.9175

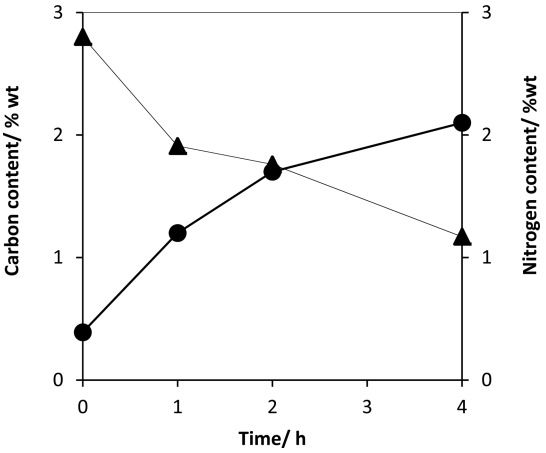

Figure 8. Evolution of the Co_3Mo_3C chemical composition after different reaction time with 60 mL min^{-1} of 75 vol % H_2 in N_2 (BOC, 99.98%) at 500 °C. (▲) Fractional carbon content and (●) fractional nitrogen content as determined by elemental analysis. The first data point corresponds to a material which was immediately cooled under the reaction flow upon attaining 500 °C.

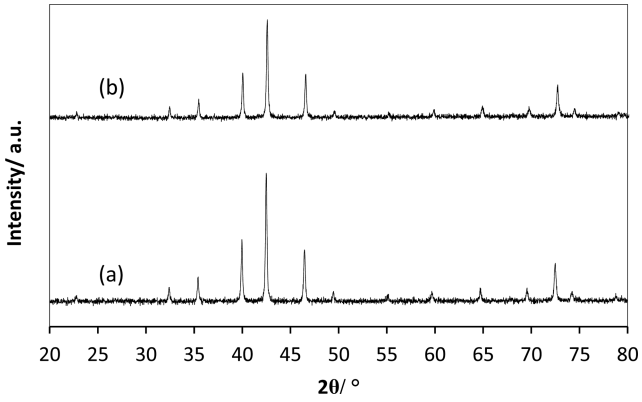

Figure 9. PXRD patterns of (a) as-prepared Co_3Mo_3C and (b) postreaction Co_3Mo_3C after 48 h of reaction using 60 mL min^{-1} of 75 vol % H_2 in N_2 (BOC, 99.98%) at 500 °C. To facilitate comparison, the two patterns are presented such as that the most intense reflections are of equivalent intensity.

nitrides, with the latter being, in general, much more reactive to, for example, water as well as oxygen. Previous work involving the reaction of Co_6Mo_6N with nitrogen-containing feeds has shown the replenishment and relocation of lattice nitrogen resulting in the formation of Co_3Mo_3N. It appears that even with a potentially reactive N_2/H_2 source under conditions known to rapidly replenish the Co_6Mo_6N system, the corresponding carbide is much less reactive, and no analogous phase transformation occurs.

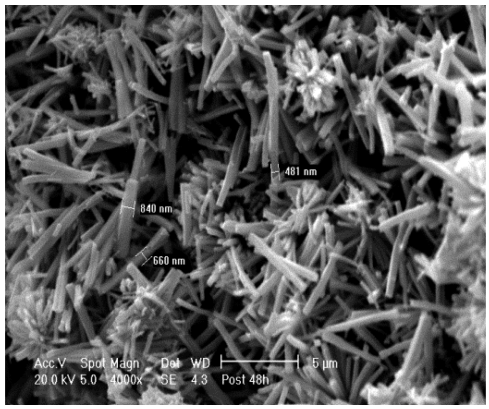

Figure 10. SEM image of Co_3Mo_3C following reaction using 60 mL min^{-1} of 75 vol % H_2 in N_2 (BOC, 99.98%) at 500 °C.

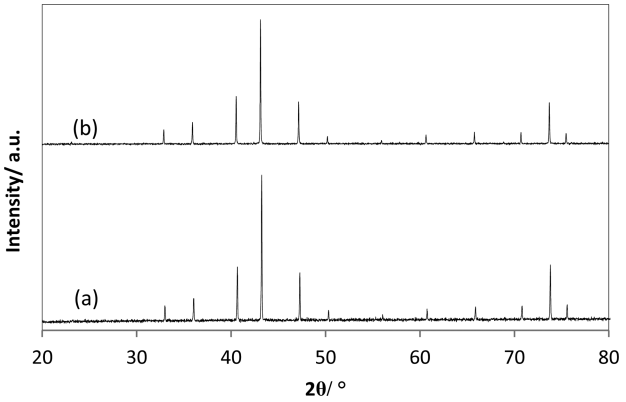

Figure 11. PXRD patterns of (a) as-prepared Co_6Mo_6C and (b) postreaction Co_6Mo_6C after 48 h of reaction using 60 mL min^{-1} of 75 vol % H_2 in N_2 (BOC, 99.98%) at 500 °C. To facilitate comparison, the two patterns are presented such as that the most intense reflections are of equivalent intensity.

The observations reported in this manuscript demonstrate that ammonia synthesis is associated with the presence of N in the 16c Wyckoff crystallographic site. Whether the origin of the activity is associated directly with the presence of this specific species or whether its presence is the result of secondary nitridation originating from the formation of ammonia has yet to be definitively established. It is also of interest that intermediate carbonitride phases do not exhibit substantially different performance from the Co_3Mo_3N phase. This might be indicative of the fact that it is only a minority of the 16c lattice N, possibly in the near surface region, which participates in the reaction. In the case of Co_6Mo_6C, the C in the 8a site seems much less reactive compared to the 16c site. This observation is to a degree consistent with the fact that upon reduction Co_3Mo_3N stops at Co_6Mo_6N. However, unlike Co_6Mo_6N,[26]

DOI: 10.1021/acssuschemeng.7b02168
ACS Sustainable Chem. Eng. 2017, 5, 9214−9222

Co_6Mo_6C does not readily transform to Co_3Mo_3N under the reaction conditions employed in this study.

CONCLUSION

In this work, we have studied the effect of composition upon the reactivity of Co_3Mo_3N, Co_3Mo_3C, and Co_6Mo_6C for ammonia synthesis reaction. Despite the isostructural nature of Co_3Mo_3N and Co_3Mo_3C, in particular, disparate performance was evident. Co_6Mo_6C, which has a closely related structure to the other two materials, was found to be inactive for ammonia synthesis under the conditions tested, while an induction time of ca. 40 min was observed in the case of Co_3Mo_3C prior to the material developing any activity. *In situ* PND and postreaction analysis revealed the substitution of carbon by nitrogen is initiated during the induction time and continues during the reaction until close to complete conversion of the carbide to the nitride. These results are consistent with the proposal of the origin of the high activity of the Co_3Mo_3N materials being the reactivity of its lattice nitrogen via a Mars–van Krevelen mechanism.

AUTHOR INFORMATION

Corresponding Author

*E-mail: Justin.Hargreaves@glasgow.ac.uk.

ORCID

Justin S. J. Hargreaves: 0000-0003-1926-9299

Author Contributions

The manuscript was written through contributions of all authors. All authors have given approval to the final version of the manuscript. These authors contributed equally.

Notes

The authors declare no competing financial interest.

ACKNOWLEDGMENTS

We are grateful to Mr. M. G. Reddy from the University of Glasgow for conducting elemental analyses and to Mr. C. Goodway, Mr. P. McIntyre, and Mr. A. Sears from the ISIS User Support Group for technical assistance with the provision and operation of the furnace and gas handling system during the *in situ* neutron diffraction experiments. J.S.J.H. wishes to acknowledge the Engineering and Physical Sciences Research Council for support through Grant EP/L02537X/1. The Science and Technologies Facilities Council is acknowledged for the allocation of beam time on the Polaris diffractometer at ISIS under experiment number RB1510336. J.L.R. is grateful to Conacyt for funding a sabbatical stay at the University of Glasgow.

REFERENCES

(1) Vojvodic, A.; Medford, A. J.; Studt, F.; Abild-Pedersen, F.; Khan, T. S.; Bligaard, T.; Nørskov, J. K. Exploring the limits: A low-pressure, low-temperature Haber–Bosch process. *Chem. Phys. Lett.* **2014**, *598*, 108–112.

(2) Nishibayashi, Y. Recent Progress in Transition-Metal-Catalyzed Reduction of Molecular Dinitrogen under Ambient Reaction Conditions. *Inorg. Chem.* **2015**, *54* (19), 9234–9247.

(3) Brown, D. E.; Edmonds, T.; Joyner, R. W.; McCarroll, J. J.; Tennison, S. R. The Genesis and Development of the Commercial BP Doubly Promoted Catalyst for Ammonia Synthesis. *Catal. Lett.* **2014**, *144* (4), 545–552.

(4) Jacobsen, C. J. H. Novel class of ammonia synthesis catalysts. *Chem. Commun.* **2000**, *12*, 1057–1058.

(5) Kojima, R.; Aika, K.-I. Cobalt molybdenum bimetallic nitride catalysts for ammonia synthesis: Part 2. Kinetic study. *Appl. Catal., A* **2001**, *218* (1–2), 121–128.

(6) Bion, N.; Can, F.; Cook, J.; Hargreaves, J. S. J.; Hector, A. L.; Levason, W.; McFarlane, A. R.; Richard, M.; Sardar, K. The role of preparation route upon the ambient pressure ammonia synthesis activity of Ni_2Mo_3N. *Appl. Catal., A* **2015**, *504*, 44–50.

(7) Kojima, R.; Aika, K.-I. Rhenium containing binary catalysts for ammonia synthesis. *Appl. Catal., A* **2001**, *209* (1–2), 317–325.

(8) McAulay, K.; Hargreaves, J. S. J.; McFarlane, A. R.; Price, D. J.; Spencer, N. A.; Bion, N.; Can, F.; Richard, M.; Greer, H. F.; Zhou, W. Z. The influence of pre-treatment gas mixture upon the ammonia synthesis activity of Co–Re catalysts. *Catal. Commun.* **2015**, *68*, 53–57.

(9) Gao, W.; Wang, P.; Guo, J.; Chang, F.; He, T.; Wang, Q.; Wu, G.; Chen, P. Barium Hydride-Mediated Nitrogen Transfer and Hydrogenation for Ammonia Synthesis: A Case Study of Cobalt. *ACS Catal.* **2017**, *7* (5), 3654–3661.

(10) Hara, M.; Kitano, M.; Hosono, H. Ru-Loaded C12A7:e– Electride as a Catalyst for Ammonia Synthesis. *ACS Catal.* **2017**, *7* (4), 2313–2324.

(11) Wang, P.; Chang, F.; Gao, W.; Guo, J.; Wu, G.; He, T.; Chen, P. Breaking scaling relations to achieve low-temperature ammonia synthesis through LiH-mediated nitrogen transfer and hydrogenation. *Nat. Chem.* **2016**, *9* (1), 64–70.

(12) Hargreaves, J. S. J. Nitrides as ammonia synthesis catalysts and as potential nitrogen transfer reagents. *Appl. Petrochem. Res.* **2014**, *4* (1), 3–10.

(13) Hargreaves, J. S. J.; McKay, D. A comparison of the reactivity of lattice nitrogen in Co_3Mo_3N and Ni_2Mo_3N catalysts. *J. Mol. Catal. A: Chem.* **2009**, *305* (1–2), 125–129.

(14) McKay, D.; Hargreaves, J. S. J.; Rico, J. L.; Rivera, J. L.; Sun, X. L. The influence of phase and morphology of molybdenum nitrides on ammonia synthesis activity and reduction characteristics. *J. Solid State Chem.* **2008**, *181* (2), 325–333.

(15) McKay, D.; Gregory, D. H.; Hargreaves, J. S. J.; Hunter, S. M.; Sun, X. Towards nitrogen transfer catalysis: reactive lattice nitrogen in cobalt molybdenum nitride. *Chem. Commun.* **2007**, *29*, 3051–3053.

(16) Hunter, S. M.; McKay, D.; Smith, R. I.; Hargreaves, J. S. J.; Gregory, D. H. Topotactic Nitrogen Transfer: Structural Transformation in Cobalt Molybdenum Nitrides. *Chem. Mater.* **2010**, *22* (9), 2898–2907.

(17) Hunter, S. M.; Gregory, D. H.; Hargreaves, J. S. J.; Richard, M.; Duprez, D.; Bion, N. A Study of $^{15}N/^{14}N$ Isotopic Exchange over Cobalt Molybdenum Nitrides. *ACS Catal.* **2013**, *3* (8), 1719–1725.

(18) Zeinalipour-Yazdi, C. D.; Hargreaves, J. S. J.; Catlow, C. R. A. Nitrogen Activation in a Mars–van Krevelen Mechanism for Ammonia Synthesis on Co_3Mo_3N. *J. Phys. Chem. C* **2015**, *119* (51), 28368–28376.

(19) Zeinalipour-Yazdi, C. D.; Hargreaves, J. S. J.; Catlow, C. R. A. DFT-D3 Study of Molecular N_2 and H_2 Activation on Co_3Mo_3N Surfaces. *J. Phys. Chem. C* **2016**, *120* (38), 21390–21398.

(20) Michalsky, R.; Avram, A. M.; Peterson, B. A.; Pfromm, P. H.; Peterson, A. A. Chemical looping of metal nitride catalysts: low-pressure ammonia synthesis for energy storage. *Chemical Science* **2015**, *6* (7), 3965–3974.

(21) Michalsky, R.; Parman, B. J.; Amanor-Boadu, V.; Pfromm, P. H. Solar thermochemical production of ammonia from water, air and sunlight: Thermodynamic and economic analyses. *Energy* **2012**, *42* (1), 251–260.

(22) Laassiri, S.; Zeinalipour-Yazdi, C. D.; Catlow, C. R. A.; Hargreaves, J. S. J. Nitrogen transfer properties in tantalum nitride based materials. *Catal. Today* **2017**, *286*, 147–154.

(23) Laassiri, S.; Zeinalipour-Yazdi, C. D.; Catlow, C. R. A.; Hargreaves, J. S. J. The potential of manganese nitride based materials as nitrogen transfer reagents for nitrogen chemical looping. *Appl. Catal., B* **2017**, na DOI: 10.1016/j.apcatb.2017.04.073.

(24) Abghoui, Y.; Garden, A. L.; Howalt, J. G.; Vegge, T.; Skúlason, E. Electroreduction of N_2 to Ammonia at Ambient Conditions on

DOI: 10.1021/acssuschemeng.7b02168
ACS Sustainable Chem. Eng. 2017, 5, 9214–9222

Mononitrides of Zr, Nb, Cr, and V: A DFT Guide for Experiments. *ACS Catal.* **2016**, *6* (2), 635−646.
(25) Abghoui, Y.; Skúlason, E. Electrochemical synthesis of ammonia via Mars-van Krevelen mechanism on the (111) facets of group III−VII transition metal mononitrides. *Catal. Today* **2017**, *286*, 78−84.
(26) Gregory, D. H.; Hargreaves, J. S. J.; Hunter, S. M. On the Regeneration of Co_3Mo_3N from Co_6Mo_6N with N_2. *Catal. Lett.* **2011**, *141* (1), 22−26.
(27) Toby, B. EXPGUI, a graphical user interface for GSAS. *J. Appl. Crystallogr.* **2001**, *34* (2), 210−213.
(28) Larson, A. C.; Von Dreele, R. B. *General Structure Analysis System (GSAS)*; Los Alamos National Laboratory Report LAUR; Los Alamos National Laboratory, 2004.
(29) Jackson, S. K.; Layland, R. C.; zur Loye, H.-C. The simultaneous powder X-ray and neutron diffraction refinement of two η-carbide type nitrides, Fe_3Mo_3N and Co_3Mo_3N, prepared by ammonolysis and by plasma nitridation of oxide precursors. *J. Alloys Compd.* **1999**, *291* (1−2), 94−101.
(30) Newsam, J. M.; Jacobson, A. J.; McCandlish, L. E.; Polizzotti, R. S. The structures of the η-carbides Ni_6Mo_6C, Co_6Mo_6C, and $Co_6Mo_6C_2$. *J. Solid State Chem.* **1988**, *75* (2), 296−304.
(31) Alconchel, S.; Sapina, F.; Martinez, E. From nitrides to carbides: topotactic synthesis of the η-carbides Fe_3Mo_3C and Co_3Mo_3C. *Dalton Transactions* **2004**, *16*, 2463−2468.
(32) Jacobsen, C. J. H.; Dahl, S.; Clausen, B. S.; Bahn, S.; Logadottir, A.; Nørskov, J. K. Catalyst Design by Interpolation in the Periodic Table: Bimetallic Ammonia Synthesis Catalysts. *J. Am. Chem. Soc.* **2001**, *123* (34), 8404−8405.
(33) Alexander, A.-M.; Hargreaves, J. S. J. Alternative catalytic materials: carbides, nitrides, phosphides and amorphous boron alloys. *Chem. Soc. Rev.* **2010**, *39* (11), 4388−4401.

DOI: 10.1021/acssuschemeng.7b02168
ACS Sustainable Chem. Eng. 2017, 5, 9214−9222